

## Low electric-field driven ultrahigh electrostrains in Sb-substituted (Na,K)NbO<sub>3</sub> lead-free ferroelectric ceramics

Jian Fu, Ruzhong Zuo, He Qi, Chen Zhang, Jingfeng Li, and Longtu Li

Citation: [Applied Physics Letters](#) **105**, 242903 (2014); doi: 10.1063/1.4904476

View online: <http://dx.doi.org/10.1063/1.4904476>

View Table of Contents: <http://scitation.aip.org/content/aip/journal/apl/105/24?ver=pdfcov>

Published by the [AIP Publishing](#)

---

### Articles you may be interested in

[The A-site Li<sup>+</sup> driven orthorhombic-tetragonal ferroelectric phase transition and evolving local structures in \(Na,K\)\(Nb,Sb\)O<sub>3</sub>-LiTaO<sub>3</sub> lead-free ceramics](#)

*Appl. Phys. Lett.* **102**, 122902 (2013); 10.1063/1.4798830

[Polarization reversal and dynamic scaling of \(Na<sub>0.5</sub>K<sub>0.5</sub>\)NbO<sub>3</sub> lead-free ferroelectric ceramics with double hysteresis-like loops](#)

*J. Appl. Phys.* **112**, 104114 (2012); 10.1063/1.4768270

[A monoclinic-tetragonal ferroelectric phase transition in lead-free \(K<sub>0.5</sub>Na<sub>0.5</sub>\)NbO<sub>3</sub>-x%LiNbO<sub>3</sub> solid solution](#)

*J. Appl. Phys.* **111**, 103503 (2012); 10.1063/1.4716027

[Effect of Ta content on the phase transition and piezoelectric properties of lead-free \(K<sub>0.48</sub>Na<sub>0.48</sub>Li<sub>0.04</sub>\)\(Nb<sub>0.995-x</sub>Mn<sub>0.005</sub>Ta<sub>x</sub>\)O<sub>3</sub> thin film](#)

*J. Appl. Phys.* **111**, 024110 (2012); 10.1063/1.3680882

[Microstructure and piezoelectric properties of lead-free \(1-x\)\(Na<sub>0.5</sub>K<sub>0.5</sub>\)NbO<sub>3</sub>-xCaTiO<sub>3</sub> ceramics](#)

*J. Appl. Phys.* **102**, 124101 (2007); 10.1063/1.2822334

---



Confidently measure down to 0.01 fA and up to 10 PΩ

KeySight B2980A Series Picoammeters/Electrometers

[View video demo](#)



## Low electric-field driven ultrahigh electrostrains in Sb-substituted (Na,K)NbO<sub>3</sub> lead-free ferroelectric ceramics

Jian Fu,<sup>1</sup> Ruzhong Zuo,<sup>1,a)</sup> He Qi,<sup>1</sup> Chen Zhang,<sup>1</sup> Jingfeng Li,<sup>2</sup> and Longtu Li<sup>2</sup>

<sup>1</sup>Institute of Electro Ceramics & Devices, School of Materials Science and Engineering, Hefei University of Technology, Hefei 230009, People's Republic of China

<sup>2</sup>State Key Laboratory of New Ceramics and Fine Processing, Department of Materials Science and Engineering, Tsinghua University, Beijing 100084, People's Republic of China

(Received 8 November 2014; accepted 6 December 2014; published online 16 December 2014)

Lead-free (Na<sub>0.52</sub>K<sub>0.48</sub>)(Nb<sub>1-y</sub>Sb<sub>y</sub>)O<sub>3</sub> (NKNS<sub>y</sub>) ferroelectric ceramics were reported to exhibit an ultrahigh electrostrain (dynamic  $d_{33}^*$  (=S/E) of 800–1100 pm/V) in a relatively low driving electric field range (1–4 kV/mm). As evidenced by *in-situ* synchrotron x-ray diffraction and dielectric measurements, the mechanism of generating large strains was ascribed to both the low-field induced reversible rhombohedral-monoclinic phase transition (1–2 kV/mm) and the enhanced domain switching (2–4 kV/mm) owing to the normal to relaxor phase transformation, which contribute to ~62% and ~38% of the total strain, respectively. The results indicate that the NKNS<sub>y</sub> compositions would have excellent potentials for applications of lead-free actuator ceramics.

© 2014 AIP Publishing LLC. [<http://dx.doi.org/10.1063/1.4904476>]

Ceramics for actuator applications need to exhibit large strains under an external electric field. Most of actuator materials have been so far mainly based on lead-based (anti) ferroelectric ceramics.<sup>1,2</sup> However, the high concentration of toxic lead oxide results in serious environmental problems and hence the research and development of lead-free alternatives have been a hot topic in recent years.

The electric field induced large strains of 0.3%–0.4% have been recently reported in some modified (Bi<sub>0.5</sub>Na<sub>0.5</sub>)TiO<sub>3</sub> (BNT) based lead-free relaxor ferroelectric ceramics.<sup>3–5</sup> It was considered that the large strain in these ceramics is mainly attributed to the reversible phase transition from an ergodic relaxor state with a nearly cubic phase to a long-range ferroelectric tetragonal phase with a large anisotropy (large *c/a* ratio).<sup>4,6</sup> However, the electric field amplitude required for achieving large strains in BNT-based ceramics is usually in the range of 6–8 kV/mm, such that the dynamic piezoelectric coefficient  $d_{33}^*$  ( $S_{\max}/E_{\max}$ ) is usually in the range of ~500–700 pm/V. The (Na,K)NbO<sub>3</sub> (NKN) based ferroelectric ceramics have also been considered as one of the most promising lead-free candidates because these materials exhibit excellent piezoelectric properties (quasi-static piezoelectric coefficient  $d_{33}$  is in the range of 200–490 pC/N) by forming the polymorphic phase boundary (PPB) that separating two ferroelectric phases,<sup>7–10</sup> similar to the traditional morphotropic phase boundary in Pb-based ferroelectric materials such as Pb(Zr,Ti)O<sub>3</sub> (PZT). Unfortunately, these lead-free NKN based PPB compositions were reported to own lower strain values than PZT-based and BNT-based perovskite systems.<sup>11–13</sup> However, compared with BNT-based lead-free ceramics, an ultralow coercive field (usually  $E_c$  less than 1 kV/mm) of NKN-based ceramics would make them promising for actuator applications.

In the present study, an ultrahigh electrostrain in a relatively low driving electric field range (dynamic  $d_{33}^*$  of 800–1100 pm/V in the field range of 1–4 kV/mm) was realized in (Na<sub>0.52</sub>K<sub>0.48</sub>)(Nb<sub>1-y</sub>Sb<sub>y</sub>)O<sub>3</sub> (NKNS<sub>y</sub>) lead-free ceramics. The mechanism of generating large strains was particularly explored in terms of a series of measurements, such as the dielectric spectroscopy, polarization and strain loops, the polarization current density loops, and *in-situ* synchrotron x-ray diffraction (XRD).

The NKNS<sub>y</sub> powders were synthesized via a conventional solid state reaction method and the as-calcined powders were mixed with 1 mol. % CuO as the sintering aid to reduce the sintering temperature. The detailed experimental procedure for preparing NKNS<sub>y</sub> ceramics could be referred elsewhere.<sup>14</sup> The as-sintered samples were ground and polished to a thickness of 0.5 mm. Silver paste was painted on both major surfaces and then fired at 600 °C. The dielectric constant as a function of temperature and frequency was measured by an LCR meter (E4980A, Agilent, Santa Clara, CA) from room temperature to 500 °C. Both polarization and strain versus electric field (P-E and S-E) loops under unipolar and bipolar electric fields were measured using a ferroelectric test system (Precision LC, Radiant Technologies, Inc., Albuquerque, NM) connected with a laser interferometric vibrometer (SP-S 120, SIOS Meßtechnik GmbH, Germany) at a fixed frequency of 1 Hz. For *in-situ* XRD measurement, gold electrodes were sputtered onto two major sides of polished samples. The XRD measurement was taken at beam line of 14B1 ( $\lambda = 1.2378 \text{ \AA}$ ) at Shanghai Synchrotron Radiation Facility.

The bipolar strain loops of NKNS<sub>y</sub> ceramics are shown in Fig. 1(a). It can be seen that most of compositions exhibit typical butterfly strain loops except for the  $y \leq 0.02$  samples, which exhibit a sprout-shaped S-E curve with an almost neglectable negative strain ( $S_{\text{neg}}$ ), because the Cu-O defect dipoles can provide a restoring force to recover the switched polarization vectors after removal of the electric field.<sup>15</sup> Moreover, the variation in shape of strain loops

<sup>a)</sup> Author to whom correspondence should be addressed. Electronic addresses: piezolab@hfut.edu.cn and rzzuo@hotmail.com. Tel.: 86-551-62905285. Fax: 0086-551-62905285.

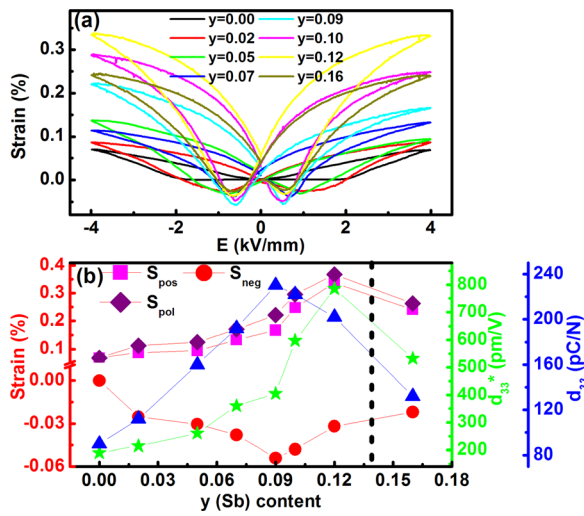


FIG. 1. (a) Strains as a function of bipolar electric fields of  $\text{NKNS}_y$  ceramics measured at room temperature at a frequency of 1 Hz and (b) the variation of  $S_{\text{pol}}$ ,  $S_{\text{pos}}$ ,  $S_{\text{neg}}$ ,  $d_{33}$ , and  $d_{33}^*$  with changing the Sb content.

with increasing  $y$  was accompanied by a distinct change of the  $S_{\text{neg}}$  and positive strain ( $S_{\text{pos}}$ ) values, as clearly seen in Fig. 1(b).  $S_{\text{neg}}$  first increases till  $y=0.09$  and then starts to decrease with further increasing  $y$ . The largest  $S_{\text{neg}}$  value just corresponds to the maximum quasi-static piezoelectric coefficient  $d_{33}$  value (230 pC/N) because both of them benefit from irreversible contributions after electric cycling. By comparison, the largest  $S_{\text{pos}}$  value ( $\sim 0.32\%$ ) appears in the  $y=0.12$  sample instead of in the  $y=0.09$  sample, which just generates the highest dynamic piezoelectric coefficient  $d_{33}^*$ . It is worthy of note that such a large electrostrain value appears in the sample ( $y=0.12$ ) with an obviously non-zero  $S_{\text{neg}}$  and a considerable quasi-static  $d_{33}$  value, which should be definitely different from the strain behavior observed in recently reported BNT based lead-free relaxor ferroelectrics.<sup>4,6</sup> For the latter, the formation of the largest electrostrain ( $S_{\text{pos}}$  or  $d_{33}^*$ ) was ascribed to the reversible nonpolar (ergodic) to polar (ferroelectric) phase transformation, such that  $d_{33}$  or  $S_{\text{neg}}$  was usually zero.<sup>4,6</sup>

To understand the mechanism of generating large strains in  $\text{NKNS}_y$  lead-free ceramics, the normalized dielectric constants ( $\epsilon_r/\epsilon_m$ ) measured at 10 kHz as a function of the normalized temperature  $T/T_m$  are shown in Fig. 2(a), where  $T_m$  is the temperature at the dielectric maxima ( $\epsilon_m$ ). One can see that the sharpness of the dielectric peak near  $T_m$  gradually decreases with increasing  $y$ , meaning that the studied compositions become more and more diffuse. Generally, the diffuseness of the phase transition can be determined from the modified Curie-Weiss law  $1/\epsilon_r - 1/\epsilon_m = (T - T_m)^{-\gamma}/C$  at  $T > T_m$ , where  $\gamma$  is the indicator of the diffuseness degree.<sup>16</sup> The  $\gamma$  values as a function of the Sb content can be then obtained by fitting the  $\ln(1/\epsilon_r - 1/\epsilon_m)$  versus  $\ln(T - T_m)$  curves, as shown in Fig. 2(b). The  $\gamma$  value of the  $y=0$  sample is 1.02, which nearly equals to the value for the pure NKN sample,<sup>17</sup> indicating that it should belong to a normal ferroelectric. This also indicates that the addition of 1 mol. % CuO did not change the dielectric diffuseness behavior of NKN ceramics. However, the  $\gamma$  value reaches 1.5 and 1.7 for the  $y=0.07$  and  $y=0.16$  samples, respectively. Similar phenomenon was

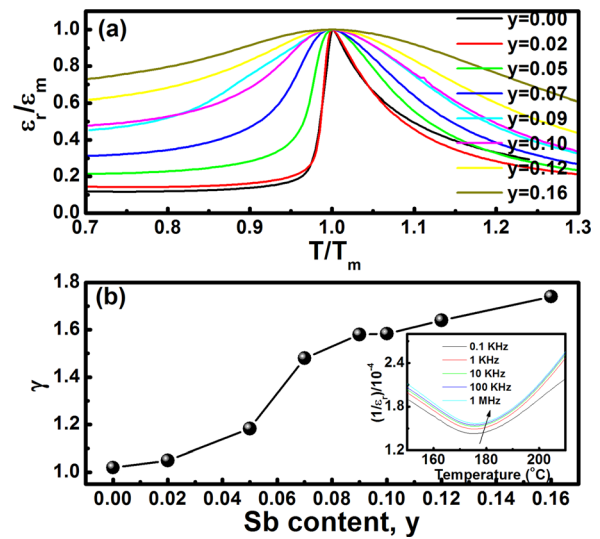


FIG. 2. (a) Normalized dielectric constants  $\epsilon_r/\epsilon_m$  at 10 kHz versus normalized temperatures  $T/T_m$  of  $\text{NKNS}_y$  ceramics, and (b) the diffuseness degree  $\gamma$  values determined by a modified Curie-Weiss law according to the  $\epsilon_r$ - $T$  curves above  $T_m$ . The inset of Fig. 1(b) shows the reciprocal dielectric constants near  $T_m$ .

also observed in  $\text{Zr}^{4+}$  doped  $\text{BaTiO}_3$  and  $\text{Ta}^{5+}$  doped NKN systems.<sup>18,19</sup> It is of note that as the Sb content is beyond 0.07, the dielectric properties start to exhibit a slight frequency dispersion beside the diffuse phase transition behavior. The calculated relaxation degree  $\Delta T_{\text{relax}}$  between two  $T_m$  values measured at 100 kHz and 100 Hz in these compositions increases gradually with increasing  $y$ . The frequency dispersion behavior of the  $y \geq 0.07$  samples is shown in the inset of Fig. 2(b) using  $y=0.12$  as an example ( $\Delta T_{\text{relax}} = 5^\circ\text{C}$  as  $y=0.12$ ). These results indicate that the substitution of  $\text{Sb}^{5+}$  for  $\text{Nb}^{5+}$  has induced an obvious normal-relaxor transformation, which corresponds to the phase structure change from orthorhombic (O) symmetry ( $y < 0.07$ ) to the coexistence of the O and rhombohedral (R) symmetries ( $y \geq 0.07$ ).<sup>14,20</sup> As a consequence, the formation of the dielectric relaxation in  $\text{NKNS}_y$  samples seems to be related to the appearance of the R phase, although it is fundamentally due to the formation of polar nanoregions (PNRs).<sup>21</sup> The disordered distribution of different ions at one or more equivalent crystallographic sites would lead to the formation of random local fields which are responsible for the growth of PNRs.<sup>22</sup> The enhancement of local random fields with increasing the Sb substitution content will result in a gradual increase of the dynamics of PNRs as well as a decrease in size of PNRs.

Fig. 3 shows P-E loops and corresponding J-E ( $dP/dt$ -E) curves for different compositions. It can be seen from Fig. 3(a) that the  $y \leq 0.02$  samples exhibit an obviously constricted and double-like hysteresis loop induced by the pinning of the domain wall motion from Cu-O defect dipoles, i.e., the ferroelectricity in these compositions is restricted.<sup>23</sup> During electric loading, a transition between a restricted ferroelectric state and a normal one would occur in  $y \leq 0.02$  samples, similar to the antiferroelectric-ferroelectric or relaxor-ferroelectric transition.<sup>24,25</sup> However, the CuO-doped NKN ceramics exhibit largely observable quasi-static  $d_{33}$  values even in  $y=0$  sample.<sup>14</sup> This is intrinsically

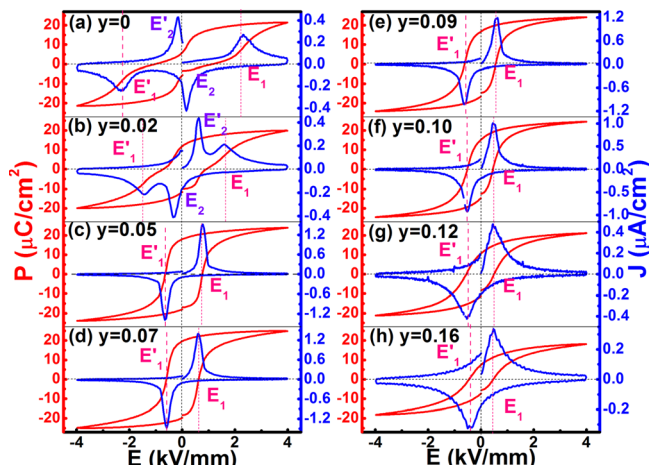


FIG. 3. The bipolar P-E loops and corresponding J-E curves of NKNS<sub>y</sub> ceramics: (a)  $y=0$ , (b)  $y=0.02$ , (c)  $y=0.05$ , (d)  $y=0.07$ , (e)  $y=0.09$ , (f)  $y=0.1$ , (g)  $y=0.12$ , and (h)  $y=0.16$ .

different from those observed in some antiferroelectrics<sup>1</sup> or in some relaxor ferroelectrics close to the ergodic and nonergodic phase boundary (or in the vicinity of their freezing temperatures).<sup>4,6,26,27</sup> The observed transition behavior in  $y \leq 0.02$  samples should be achieved by reversible domain switching, thus generating the forward-switching peaks  $E_1$  (and  $E_1'$ ) and backward-switching peaks  $E_2$  (and  $E_2'$ ).<sup>15</sup> As  $y > 0.02$ , the backward-switching current peaks  $E_2$  and  $E_2'$  start to disappear and only a single polarization current peak corresponding to the normal domain switching was observed during electric loading, as shown in Figs. 3(c)–3(h). The result implies that the pinning effect of domain walls does not work any more because of gradually increased domain switching dynamics as mentioned above. Moreover, the decrease of the coercive fields  $E_c$  (denoted as  $E_1$  in Fig. 1) further confirms that the substitution of  $Sb^{5+}$  makes the domain switching easier. It can be also seen that the saturated polarization  $P_{max}$  values do not change obviously as  $y \geq 0.07$  (except for the  $y = 0.16$  sample because of a small amount of secondary phases based on the solubility limit of  $Sb^{5+}$  in the NKN lattice).<sup>14</sup> That is to say, all relaxor compositions are ferroelectric in nature. Therefore, a long-range ferroelectric ordering can be electrically induced in these compositions, accompanied by an obvious domain switching process. In addition to the domain switching during loading, a phase structural transition from R phase or O phase to monoclinic (M) phase was already confirmed in our previous work by means of high-resolution synchrotron XRD.<sup>20</sup> As known, the useful electrostrain value (i.e.,  $S_{pos}$ ) generated in a ferroelectric composition generally equals to the amount of poling strains ( $S_{pol}$ ) minus the irreversible strain parts (i.e.,  $S_{neg}$ ). The enhanced domain switching and electric field induced O-M and R-M phase transitions would significantly contribute to the increase of the  $E_{pol}$  value with increasing the Sb content (see Fig. 1(b)). By comparison, the reversibility of R-M phase transition<sup>20</sup> will lead to the minimum  $S_{neg}$  value. The electric field induced irreversible O-M phase transition<sup>20</sup> would dominantly contribute to the observed  $S_{neg}$  in Fig. 1, which was thus found to gradually decrease with increasing  $y$  owing to the reduction of the O phase amount within the O-R phase coexistence zone. As a result, both  $S_{pos}$

and  $d_{33}^*$  values monotonously increase with increasing the Sb content, reaching 0.32% and 800 pm/V, respectively, at  $y = 0.12$ .

Fig. 4(a) shows the evolution of (222) pseudocubic reflections for the  $y = 0.12$  sample under different external electric fields. It is obvious that the  $y = 0.12$  virgin sample basically belongs to an R phase (as  $E = 0$ –0.5 kV/mm), as characterized by two split (222)/(22-2) diffraction lines. As the applied electric field is above 1 kV/mm, an M phase with three featured diffraction peaks  $(-402)/(042)/(402)$  can be electrically induced. This electric field induced new phase should be an  $M_B$  phase with a Cm symmetry, as sketched in Fig. 4(b). The polar axis of the Cm symmetry lies close to the  $[-201]_M$  direction, i.e., close to the  $[111]_R$  axis. Although the electric field magnitude is further increased, no obvious domain switching can be detected until  $E > 2$  kV/mm. As the electric field is above 2 kV/mm, a distinct increase of the peak intensity ratio between  $(-402)/(402)$  planes can be seen, indicating that poling process has induced a considerable domain switching behavior along its polar axis direction. Similar domain switching behavior was also observed in ferroelectrics with other symmetries such as T and R phases, in which the intensity ratios between (002)/(200) planes and (111)/(1-1) increased after poling, respectively.<sup>28</sup> Figs. 4(c) and 4(d) show the unipolar strain loops and the corresponding strain values of the  $y = 0.12$  virgin samples under various electric field amplitudes. Because the amount of O phase is very low in the  $y = 0.12$  sample, the contribution of irreversible O-M phase transition to the strain during loading is negligible. It can be seen that the generated strains show a drastic increase in the field range of 1–2 kV/mm, and then continue to increase a little slowly after 2 kV/mm, as can be seen from the slope of the strain versus electric field (S/E) curve (Fig. 4(d)). Before 1 kV/mm, a very small contribution to the strain should be ascribed to the electrostrictive effect. As discussed above concerning the *in-situ* XRD results, a large contribution of  $\sim 62\%$  of the total strain in the field range of 1–2 kV/mm should be attributed to the electric field induced reversible R-M phase transition. Further domain switching

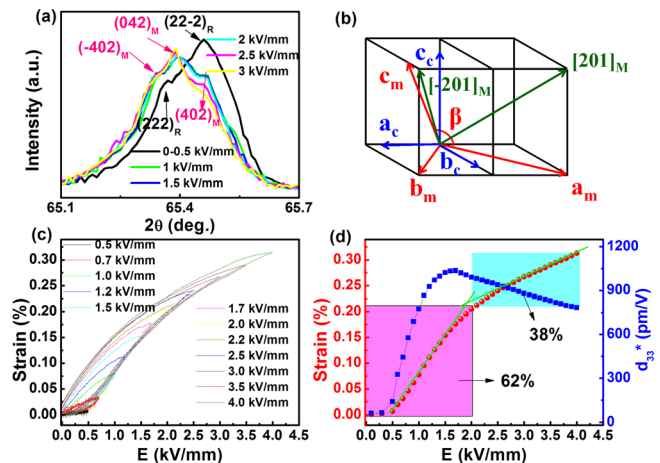


FIG. 4. (a) The (222) pseudocubic reflection lines for the  $y = 0.12$  sample under different external electric fields, (b) the sketch of the unit cell of  $M_B$  phase with Cm symmetry, (c) unipolar S-E curves of the  $y = 0.12$  sample under different external electric fields, and (d) the generated strains and dynamic  $d_{33}^*$  values under each driving electric field.

as  $E > 2$  kV/mm would lead to the left  $\sim 38\%$  of the total strain. Interestingly, because the field induced R-M phase transition easily occurs under a relatively low electric field ( $\sim 1$  kV/mm), an ultrahigh dynamic piezoelectric coefficient  $d_{33}^*$  value of  $\sim 1100$  pm/V can be obtained. In a wide field range of 1–4 kV/mm, a  $d_{33}^*$  value as high as  $\sim 800$  pm/V can be maintained. As  $E = 4$  kV/mm, the generated strain reaches  $\sim 0.32\%$ , which is comprised the low-field phase transition contribution ( $\sim 0.2\%$ ) and the enhanced domain switching contribution ( $\sim 0.12\%$ ). Such a large domain switching contribution was rarely observed in conventional PZT-based ceramics.<sup>2</sup> It should be closely correlated in the current study with the miniaturization of domain structures accompanied by the Sb induced normal to relaxor transformation. Compared with BNT-based lead-free large-strain ferroelectric ceramics, the Sb substituted NKN ceramics in the current study should have more potentials for actuator applications because an extremely low driving electric field is required for generating a large dynamic  $d_{33}^*$  up to  $\sim 1100$  pm/V.

In summary, low electric field induced large strain and its corresponding structural mechanism in  $\text{NKNS}_y$  ceramics were investigated. An ultrahigh electrostrain of  $\sim 0.32\%$  can be generated under an electric field of 4 kV/mm in the  $y=0.12$  sample. Such a large dynamic  $d_{33}^*$  value of 800–1100 pm/V can be maintained in a wide field range of 1–4 kV/mm. The mechanism of generating large strains in  $\text{NKNS}_y$  ceramics was ascribed to the low-field induced R-M phase transition (1–2 kV/mm) and the enhanced domain switching, which contribute to  $\sim 62\%$  and  $\sim 38\%$  of the total strain, respectively. The reversibility of R-M phase transition was believed to produce the minimum irreversible strain. The Sb substitution induced normal to relaxor phase transition enhances the dynamics of domain switching. The results indicate that the  $\text{NKNS}_y$  compositions would have excellent potentials for applications of lead-free actuator ceramics.

The authors would like to thank Shanghai Synchrotron Radiation Source for use of the synchrotron radiation facilities. Financial support from the National Natural Science Foundation of China (Grant Nos. U1432113, 51402079, and 51332002) is gratefully acknowledged.

- <sup>1</sup>S. E. Park, M. J. Pan, K. Markowski, S. Yoshikawa, and L. E. Cross, *J. Appl. Phys.* **82**, 1798 (1997).
- <sup>2</sup>H. Kungl, R. Theissmann, M. Knapp, C. Baetz, H. Fuess, S. Wagner, T. Fett, and M. J. Hoffmann, *Acta Mater.* **55**, 1849 (2007).
- <sup>3</sup>P. Jarupoom, E. Patterson, B. Gibbons, G. Rujijanagul, R. Yimnirun, and D. Cann, *Appl. Phys. Lett.* **99**, 152901 (2011).
- <sup>4</sup>W. Jo, R. Dittmer, M. Acosta, J. D. Zang, C. Groh, E. Sapper, K. Wang, and J. Rodel, *J. Electroceram.* **29**, 71 (2012).
- <sup>5</sup>A. Ullah, C. W. Ahn, A. Ullah, and I. W. Kim, *Appl. Phys. Lett.* **103**, 022906 (2013).
- <sup>6</sup>H. Simons, J. E. Daniels, J. Glaum, A. J. Studer, J. L. Jones, and M. Hoffman, *Appl. Phys. Lett.* **102**, 062902 (2013).
- <sup>7</sup>S. J. Zhang, R. Xia, T. R. Shrout, G. Z. Zang, and J. F. Wang, *J. Appl. Phys.* **100**, 104108 (2006).
- <sup>8</sup>R. Z. Zuo, J. Fu, and D. Y. Lv, *J. Am. Ceram. Soc.* **92**, 283 (2009).
- <sup>9</sup>Y. S. Sung, S. Baik, J. H. Lee, G. H. Ryu, D. Do, T. K. Song, M. H. Kim, and W. J. Kim, *Appl. Phys. Lett.* **101**, 012902 (2012).
- <sup>10</sup>X. P. Wang, J. G. Wu, D. Q. Xiao, J. G. Zhu, X. J. Cheng, T. Zheng, B. Y. Zhang, X. J. Lou, and X. J. Wang, *J. Am. Chem. Soc.* **136**, 2905 (2014).
- <sup>11</sup>R. Z. Zuo, J. Fu, G. Z. Yin, X. L. Li, and J. Z. Jiang, *Appl. Phys. Lett.* **101**, 092906 (2012).
- <sup>12</sup>J. J. Zhou, K. Wang, F. Li, J. F. Li, X. W. Zhang, and Q. M. Wang, *J. Am. Ceram. Soc.* **96**, 519 (2013).
- <sup>13</sup>K. Yan and X. B. Ren, *J. Phys. D: Appl. Phys.* **47**, 015309 (2014).
- <sup>14</sup>R. Z. Zuo, J. Fu, D. Y. Lv, and Y. Liu, *J. Am. Ceram. Soc.* **93**, 2783 (2010).
- <sup>15</sup>J. Fu and R. Z. Zuo, *J. Appl. Phys.* **112**, 104114 (2012).
- <sup>16</sup>K. Uchino and S. Nomura, *Ferroelectr., Lett. Sect.* **44**, 55 (1982).
- <sup>17</sup>H. L. Du, W. C. Zhou, D. M. Zhu, L. Fa, S. B. Qu, Y. Li, and Z. B. Pei, *J. Am. Ceram. Soc.* **91**, 2903 (2008).
- <sup>18</sup>Y. F. Chang, Z. P. Yang, D. F. Ma, Z. H. Liu, and Z. L. Wang, *J. Appl. Phys.* **104**, 024109 (2008).
- <sup>19</sup>X. G. Tang, K. H. Chw, and H. L. W. Chan, *Acta Mater.* **52**, 5177 (2004).
- <sup>20</sup>J. Fu, R. Z. Zuo, and X. Y. Gao, *Appl. Phys. Lett.* **103**, 182907 (2013).
- <sup>21</sup>A. A. Bokov and Z. G. Ye, *J. Mater. Sci.* **41**, 31 (2006).
- <sup>22</sup>V. V. Shvartsman, A. L. Kholkin, A. Orlova, D. Kiselev, A. A. Bogomolov, and A. Sternberg, *Appl. Phys. Lett.* **86**, 202907 (2005).
- <sup>23</sup>V. S. Postnikov, V. S. Pavlov, and S. K. Turkov, *J. Phys. Chem. Solids* **31**, 1785 (1970).
- <sup>24</sup>J. Glaum, H. Simons, M. Acosta, and M. Hoffman, *J. Am. Ceram. Soc.* **96**, 2881 (2013).
- <sup>25</sup>Y. H. Xu, W. Hong, Y. J. Feng, and X. L. Tan, *Appl. Phys. Lett.* **104**, 052903 (2014).
- <sup>26</sup>W. L. Zhao, R. Z. Zuo, J. Fu, and M. Shi, *J. Eur. Ceram. Soc.* **34**, 2299 (2014).
- <sup>27</sup>W. L. Zhao, R. Z. Zuo, D. G. Zheng, and L. T. Li, *J. Am. Ceram. Soc.* **97**, 1855 (2014).
- <sup>28</sup>R. Guo, L. E. Cross, S. E. Park, B. Noheda, D. E. Cox, and G. Shirane, *Phys. Rev. Lett.* **84**, 5423 (2000).